Resonance Raman Studies of Blue Copper Proteins: Effect of Temperature and Isotopic Substitutions. Structural and Thermodynamic Implications†

David F. Blair,[1a] Gary W. Campbell,[1a] Jon R. Schoonover,[1c] Sunney I. Chan,*[1a] Harry B. Gray,*[1a] Bo G. Malmstrom,*[1d,f] Israel Pecht,*[1e,g] Basil I. Swanson,*[1b] William H. Woodruff,*[1c,j] W. K. Cho,[1a,h] Ann M. English,[1a,i] Herbert A. Fry,[1b] Vanessa Lum,[1a] and K. A. Norton[1c]

Contribution from the Inorganic and Structural Chemistry Group (INC-4), Isotope and Nuclear Chemistry Division, Los Alamos National Laboratories, Los Alamos, New Mexico 87545, Contribution No. 6990 from the Arthur Amos Noyes Laboratory of Chemical Physics, California Institute of Technology, Pasadena, California 91125, the Department of Biochemistry and Biophysics, University of Goteborg and Chalmers Institute of Technology, S-412 96, Goteborg, Sweden, and the Department of Chemical Immunology, The Weizmann Institute of Science, Rehovot, Israel. *Received October 18, 1984*

Abstract: Resonance Raman spectra of the single-copper blue proteins azurin (from the bacteria *Pseudomonas putida*, *Pseudomonas aeruginosa*, *Iwasaki sp.*, *Bortadella pertussis*, *Bortadella bronchiseptica*, and *Alcaligenes faecalis*), plastocyanin (from French bean and spinach), and stellacyanin (from the Japanese and Chinese lacquer trees *Rhus vernicifera*) and the multicopper oxidases laccase (from the fungus *Polyporus versicolor* and the Japanese and Chinese lacquer trees), ascorbate oxidase (from zucchini squash), and ceruloplasmin (from human blood serum) are reported. Cryoresonance Raman observations (10–77 K) are reported for selected azurins, stellacyanin, the plastocyanins, and the laccases. Isotope studies employing $^{63}Cu/^{65}Cu$ and H/D substitution are reported for selected azurins and stellacyanin, allowing identification of modes having significant copper–ligand (Cu–L) stretch and internal ligand deformation character. Principal conclusions include the following. The only Cu–L stretching mode near 400 cm^{-1} is the Cu–S(Cys) stretch, and the remainder of the elementary motions near this frequency are internal ligand deformations. All the observed modes near 400 cm^{-1} are highly mixed, and most derive their intensity from their fractional Cu–S(Cys) stretching character. The Cu–N(His) stretching motions are best identified with the ubiquitous peak(s) near 270 cm^{-1}, although in azurin these modes have contributions from other coordinates. Internal histidine and cysteine motions contribute to the features near 400 cm^{-1}. Even with the improved resolution and signal-to-noise forthcoming at 10 K, the resonance Raman excitation profiles show negligible variation of relative intensities among the resonance-enhanced modes of a given protein. This is consistent with a single resonant electronic chromophore (viz., $RS^-(Cys) \rightarrow Cu^{2+}$ LMCT) and extremely facile vibrational dephasing or other damping processes in the electronically excited state. Temperature effects upon the spectra suggest a significant temperature-dependent structure change at the plastocyanin active site, and a more subtle one in azurin. It is shown that the Cu–S(Cys) stretching frequency is closely correlated to the electron-transfer exothermicity for several proteins, thereby indicating that the reduction potential can be fine-tuned by the effects of polypeptide backbone structure on the copper–sulfur bond distance and the copper–ligand field.

The blue copper proteins, including the simple one-copper blue proteins and the multicopper oxidases which contain a blue ("type 1") copper site, are now widely recognized to have a number of remarkable spectroscopic and chemical properties. These have been the subject of active investigation for some years[2,3] and include inter alia intense low-energy electronic absorption features in the visible spectrum (see Figure 1), very low-energy Cu^{2+}–ligand field transitions, small copper hyperfine coupling constants in the Cu^{2+} EPR spectra, unusually strong (and variable) oxidizing power for the Cu^{2+} oxidation state, and facile electron-transfer dynamics.[4,5]

The X-ray crystal structures of poplar plastocyanin and two azurins have recently been determined.[6-8] The structure of the copper site of poplar plastocyanin is shown in Figure 1. The ligation of copper includes two histidine imidazole nitrogens and a cysteine sulfur defining a trigonal plane, the copper atom slightly above this plane, and a very long apical distance to methionine sulfur. Complementary structural studies of a number of blue copper proteins have been performed by EXAFS.[9-11] Accordingly, many of the spectroscopic and chemical observations are interpretable on the basis of the more obvious features of these now-known structures.

On the other hand, many important observations remain incompletely understood despite intense and continuing investigation. Cases in point include the relationships between the thermochemical parameters for the electron-transfer reactions and the energies of ligand-field transitions,[12] certain aspects of the charge-transfer spectra including the virtual absence of temperature dependence,[13] the resonance Raman spectra and their temperature dependence for ostensibly similar proteins,[14] and the

† Dedicated to the memory of Eraldo Antonini.

(1) (a) California Institute of Technology. (b) Los Alamos National Laboratories. (c) University of Texas at Austin. (d) University of Goteborg. (e) Weizmann Institute of Science. (f) Sherman Fairchild Distinguished Scholar, California Institute of Technology, 1980–1981. (g) Sherman Fairchild Distinguished Scholar, California Institute of Technology, 1982. (h) Present address: Department of Physics, Chinese University of Hong Kong, Shaitin, N.T., Hong Kong. (i) Present address: Department of Chemistry, Concordia University, Montreal, Quebec, Canada. (j) Present address: Los Alamos National Laboratories.

(2) Malkin, R.; Malmstrom, B. G. *Adv. Enzymol.* **1970**, *33*, 177–182.
(3) Fee, J. A. **1975**, *Struct. Bonding (Berlin) 23*, 1–53.
(4) Gray, H. B. *Adv. Inorg. Biochem.* **1980**, *2*, 1.
(5) Spiro, T. G., *Met. Ions Biol.* **1981**, *3*, 1.
(6) Freeman, H. C. *Coord. Chem.* **1981**, *21*, 1. Guss, J. M.; Freeman, H. C. *J. Mol. Biol.* **1983**, *169*, 521. Atomic coordinates obtained from Brookhaven Protein Data Bank.
(7) Adman, E. T.; Stenkamp, R. E.; Sieker, L. C.; Jensen, L. H. *J. Mol. Biol.* **1978**, *123*, 35–40. Adman, E. T.; Jensen, L. H. *Isr. J. Chem.* **1981**, *21*, 8–13. Atomic coordinates obtained from Brookhaven Protein Data Bank.
(8) Norris, G. E.; Anderson, B. F.; Baker, E. N. *J. Mol. Biol.* **1983**, *165*, 501.
(9) Scott, R. A.; Hahn, J. E.; Doniach, S.; Freeman, H. C.; Hodgson, K. O. *J. Am. Chem. Soc.* **1982**, *104*, 5364–5369.
(10) Tulius, T. D.; Frank, P.; Hodgson, K. O. *Proc. Natl. Acad. Sci. U.S.A.* **1978**, *75*, 4069–4074.
(11) Peisach, J.; Powers, L.; Blumberg, W. E.; Chance, B. *Biophys. J.* **1982**, *38*, 277.
(12) Gray, H. B.; Malmstrom, B. G. *Comments Inorg. Chem.* **1983**, *2*, 203.
(13) Solomon, E. I.; Hare, J. W.; Dooley, D. M.; Dawson, J. H.; Stephens, P. J.; Gray, H. B. *J. Am. Chem. Soc.* **1980**, *102*, 168–173.
(14) Woodruff, W. H.; Norton, K. A.; Swanson, B. I.; Fry, H. A. *Proc. Natl. Acad. Sci. U.S.A.* **1984**, *81*, 1263.

0002-7863/85/1507-5755$01.50/0

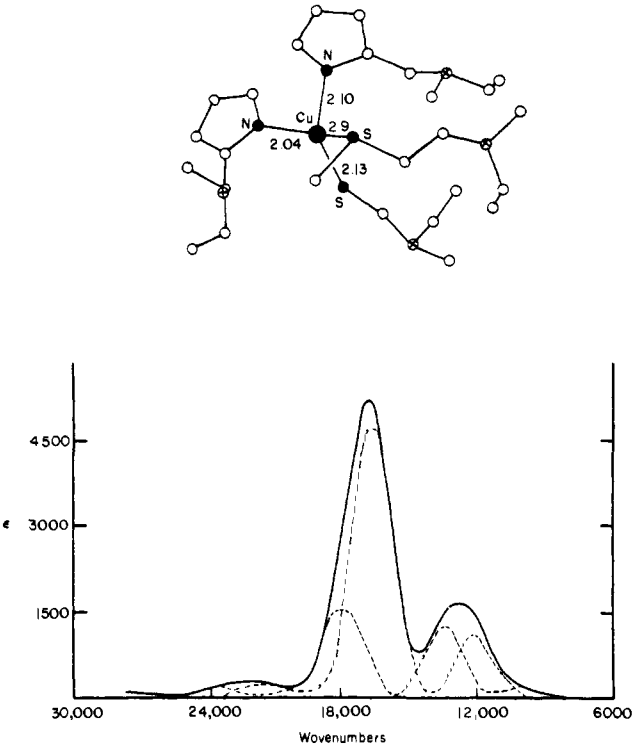

Figure 1. (Top) Structure of the copper site of poplar plastocyanin, adapted from ref 6. The atoms denoted x are the α-carbon atoms of the polypeptide backbone. (Bottom) The visible absorption spectrum of bean plastocyanin at 35 K (solid line) and the Gaussian resolution (dashed lines), adapted from ref 13.

unobservability by EXAFS of the Cu–S(Met) bond distance in plastocyanin.[9] These properties and others may be influenced by structural parameters that are beyond the present ability of X-ray methods to elucidate or alternatively by dynamical effects to which determinations of average structure are insensitive.

A number of resonance Raman (RR) studies of blue copper proteins have been reported.[14-22] It is evident from these investigations, particularly those undertaken under cryogenic conditions[14,18,20-22] that the RR spectra are more sensitive to differences among the structures and the quantum dynamics of the proteins than are spectra derived from more commonly applied spectroscopies (notably electronic and ESR) and hence potentially contain more information. For example, plastocyanin and azurin are quite similar by most spectroscopic criteria and also by existing X-ray crystallographic observations of the structures of the proteins and their active sites. However, the spectra of azurin and plastocyanin are considerably dissimilar with respect to the number of RR modes observed, their frequencies, relative intensities, line shapes, and temperature dependences.[14]

Satisfactory structural interpretation of blue copper RR spectra has so far not been available. Vibrational analyses based upon a five-atom CuL_4 model have been helpful in understanding the limits that the RR results place on Cu–L binding[19,20] and in interpreting isotope shifts.[20] Structurally, however, the five-atom model clearly contains insufficient detail. Considerable progress can be made toward understanding the structural significance of the RR spectra by careful examination of a wide variety of protein systems. Recent cryogenic resonance Raman results[14,18,20] have pointed to substantially revised interpretation of the blue copper RR spectra. In the present study, we report cryoresonance Raman spectra for a number of blue copper proteins: the single-copper blue proteins azurin, plastocyanin, and stellacyanin and the multicopper oxidases laccase, ascorbate oxidase, and ceruloplasmin. In addition, species comparisons are made for azurin (*Pseudomonas putida*, PP; *Pseudomonas aeruginosa*, PA; *Iwasaki sp.*, IS; *Bortadella pertussis*, BP; *Bortadella bronchiseptica*, BB; and *Alcaligenes faecalis*, AF), plastocyanin (*Phaseolus vulgaris* and *Spinacea oleracea*), and laccase (*Polyporus versicolor* and *Rhus vernicifera*). We have also undertaken isotope studies ($^{63}Cu/^{65}Cu$ and H/D) of azurins to allow refinement of the vibrational assignments in this protein. In addition, we have examined the effects of temperature on the RR spectra of several of the proteins.

On the basis of our studies, we have proposed an assignment scheme for a number of the RR features of blue proteins. The present results show that a reliable vibrational analysis must have as its basis adequate vibrational analysis of the ligands themselves. Even in the absence of formal analysis, however, the present work does allow some general features of structure, vibrational dynamics, and structure–function relationships to be elucidated.

Experimental Section

Protein Preparations. Samples for RR were prepared by dialysis of the metalloprotein into the desired buffer and subsequent concentration by ultrafiltration or lyophilization. The protein was diluted to a final concentration of ca. 2 mM in type 1 copper (absorbance ca. 1 mm^{-1} at λ_{max} ~600 nm). The A_{600}/A_{280} absorbance ratios for the proteins remained constant through this procedure when care was taken to perform the dissolution step in the cold (4 °C). Samples were then frozen and stored at −20 °C until needed for RR measurements. For experiments in which an internal intensity standard was required, portions of the original sample were diluted with an equal amount of 1.0 M Na_2SO_4 at the time of measurement.

Azurins were prepared by established procedures.[31,32] Purification was by gel chromatography on a Sephadex G-25 column (pH 7.0, 0.01 M potassium phosphate buffer) until the ratio of A_{625}/A_{280} was 0.52. Spinach (*Spinacea oleracea*) plastocyanin was purified by a modified version of the method of Katoh;[33] modification included precipitation of proteins from 0.05 M tris(hydroxymethyl)aminomethane buffer, pH 8.0, by acetone. The plastocyanin was purified on a Whatman DE-52 ion-exchange column (pH 7.0, 0.1 M potassium phosphate buffer) and chromatographed on Sepehadex G-50 until an A_{597}/A_{278} ratio of 1.2 was obtained. French bean (*Phaseolus vulgaris*) plastocyanin[34] (A_{597}/A_{280} = 1.0), *Polyporus versicolor* (fungal) laccase A[35] (A_{280}/A_{610} = 16.1), and *Curburbita pepomedullosa* ascorbate oxidase[36] (A_{280}/A_{610} = 25.6) were isolated by the previously described methods. Human ceruloplasmin from fresh serum was obtained by using a modification of the method of Rydén and Björk[37] (A_{610}/A_{280} = 0.45). The procedure of Reinhammar[38] or modifications thereof[39] were used to purify Japanese and Chi-

(15) Siiman, O.; Young, N. M.; Carey, P. R. *J. Am. Chem. Soc.* **1974**, *96*, 5583–5588. Siiman, O.; Young, N. M.; Carey, P. R. *J. Am. Chem. Soc.* **1976**, *98*, 744–749.
(16) Miskowski, V. N.; Tang, S.-P. W.; Sprio, T. G.; Shapiro, E.; Moss, T. H. *Biochemistry* **1975**, *14*, 1244–1249.
(17) Ferris, N. S.; Woodruff, W. H.; Tennent, D. L.; McMillin, D. R. *Biochem. Biophys. Res. Commun.* **1979**, *88*, 288–293.
(18) Woodruff, W. H.; Norton, K. A.; Swanson, B. I.; Fry, H. A. *J. Am. Chem. Soc.* **1983**, *105*, 657–662.
(19) Thamman, T. J.; Frank, P.; Willis, L. C.; Loehr, T. M. *Proc. Natl. Acad. Sci. U.S.A.* **1981**, *79*, 6396–6401.
(20) Nestor, L. P.; Larrabee, J. A.; Woolery, G.; Reinhammer, B.; Spiro, T. G. *Biochemistry* **1984**, *23*, 1084.
(21) Blair, D. F.; Campbell, G. W.; Lum, V.; Martin, C. T.; Gray, H. B.; Malmstrom, B. G.; Chan, S. I. *J. Inorg. Biochem.* **1983**, *19*, 65.
(22) Blair, D.; Campbell, G. W.; Cho, W.; Fry, H. A.; Lum, V.; Norton, K. A.; Chan, S. I.; Gray, H. B.; Malmstrom, B. G.; Pecht, I.; Swanson, B. I.; Woodruff, W. H. *Inorg. Chim. Acta* **1983**, *79*, 51–56.
(23) Heller, E. J. *Acc. Chem. Res.* **1981**, *14*, 368.
(24) Heller, E. J.; Sundberg, R. L.; Tannor, D. *J. Phys. Chem.* **1982**, *86*, 1822.
(25) Tannor, D.; Heller, E. J., personal communication.
(26) McMillin, D. C.; Morris, M. C. *Proc. Natl. Acad. Sci. U.S.A.* **1981**, *78*, 65–70.
(27) Woodruff, W. H.; Miskowski, V. M.; Gray, H. B. **1981**, *J.B.S. Lett.* *69*, 175.
(28) Roberts, J. E.; Brown, T. G.; Hoffman, B. M.; Peisach, J. *J. Am. Chem. Soc.* **1980**, *102*, 825.
(29) Herschbach, D. R.; Laurie, V. W. *J. Chem. Phys.* **1961**, *35*, 458.
(30) Taniguchi, V. T.; Malmstrom, B. G.; Anson, F. C.; Gray, H. B. *Proc. Natl. Acad. Sci. U.S.A.* **1982**, *79*, 2287. Taniguchi, V. T.; Sailasata-Scott, N.; Anson, F. C.; Gray, H. B. *Pure Appl. Chem.* **1980**, *52*, 2275.
(31) Rosen, P.; Pecht, I. *Biochemistry* *15*, 775–780.
(32) Ambler, R. P.; Brown, L. M. *Biochem. J.* **1976**, *21*, 5.
(33) (a) Katoh, S. *Methods Enzymol.* **1981**, *23*, 1. (b) Brand, J. G.; Norton, K. A., unpublished results.
(34) Wells, J. R. E. *Biochem. J.* **1965**, *97*, 228.
(35) Fåhraeus, G.; Reinhammar, B. *Acta Chem. Scand.* **1967**, *21*, 5.
(36) Dooley, D. M.; Dawson, J. H.; Stephens, P. J.; Gray, H. B. *Biochemistry* **1981**, *20*, 2024.
(37) Rydén, L.; Björk, J. *Biochemistry* **1976**, *15*, 3411.

nese *Rhus vernicifera* (tree) laccase (A_{280}/A_{614} = 15.4) and stellacyanin (A_{280}/A_{604} = 5.8).

For deuterium-exchange experiments, azurin solutions (ca. 1 mM in protein, 10 mM acetate, pH 6.0) were lyophilized followed by resuspension in D_2O. Samples were incubated in D_2O for at least 24 h at 4 °C prior to obtaining RR spectra. Copper was removed from azurin by dialysis against 0.5 M KCN for 2 days at 4 °C. Cyanide ions and copper were then removed from the protein solution by dialysis against acetate buffer for 6 h. The samples were reconstituted with isotopically pure ^{65}Cu or ^{63}Cu (Oak Ridge National Laboratories) by overnight dialysis against 5 mM solutions of the appropriate copper isotope in 20 mM acetate, pH 6.0. Excess copper was removed by dialysis against 20 mM acetate, pH 6.0, for 6 h.

Spectroscopic Measurements. RR spectra were obtained by using one of three spectrometers: a SPEX 1403 equipped with a thermoelectrically cooled RCA C31034A photomultiplier tube, a Princeton Applied Research Model 1112 photon-counting system, and a Nicolet 1180E Raman data system; a SPEX Ramalog EU equipped with a cooled RCA 31034A photomultiplier tube, an ORTEC 9300 series photon counter, and a Nicolet 1180E Raman data system; or a SPEX 14024 spectrometer equipped with 2400 lines/mm holographic gratings, a thermoelectrically cooled Hammamatsu R955 photomultiplier tube, and a SPEX SCAMP data system. Laser excitation was provided by a Spectra-Physics 171-01 Kr^+ laser (413.1, 568.2, 647.1, and 674.6 nm), or a Coherent Radiation 590 or Spectra-Physics 375A tunable dye laser (Rhodamine 590 or Rhodamine 610 dye, 560–650 nm) pumped by a Spectra-Physics 171-19 Ar^+ laser. Spectra were typically obtained with spectral slit widths of 3–5 cm^{-1} and digital resolution of 0.2–0.4 cm^{-1}. Spectral scan rates were 1–2 cm^{-1} s^{-1} with no analog time constant employed. Typical signal averaging utilized 9 or 16 coadded scans. The durability of the sample could be assessed during acquisition of a spectrum of observing the quality of any given scan. In some cases, up to 100 scans were averaged together.

For the 300, 277, and 77 K experiments, laser power was maintained at approximately 30 mW at the sample. Sample temperature was controlled by immersion in liquid nitrogen (77 K), by a stream of cold, dry air (277 K), or by contact with the ambient (nominally 300 K). Samples were contained in melting point capillaries, and standard 90° scattering geometry was employed. In these experiments, some samples, especially fungal laccase, were observed to bleach after prolonged periods of irradiation. Visual inspection of the samples for photobleaching as well as comparison of scans taken near the beginning and the end of data acquisition periods revealed no evidence for loss of sample integrity.

For the 10–30 K experiments, the cryogenic apparatus consisted of an Air Products Displex cryostat with a Lakeshore Cryogenics silicon diode controller. Laser power was typically 10 mW at the cryostat window. Temperatures quoted refer to nominal cryotip temperatures; the actual sample temperature at the Raman scattering point must be higher due to local heating by the laser. Experiments near the melting point of water showed that a nominal cryotip temperature of 244 K correspond to a temperature at the Raman scattering point of 270 K with a laser power of 8 mW (a satisfactory internal temperature reference for Stokes/anti-Stokes intensity ratios in protein solutions at very low temperatures is presently lacking). The sample cuvettes were cylindrical, 5-mm diameter by 1-mm path length, with windows fashioned from Suprasil flats. The cryotip was fitted with a copper cold finger which held the cuvette with the maximum area in contact with the copper and only one window exposed. Good thermal contact was maintained by Dow-Corning silicone heat-sink compound. The angle of incidence of the laser beam upon the cuvette window was approximately 60°, the polarization was sagittal, and the Raman scattering was collected in the plane of incidence at 90° to the incident beam.

Visible and ultraviolet spectra were obtained by using Cary 17DX or 219 spectrophotometers. Measurements of pH were made by using a Radiometer PHM-64 research pH meter.

Results

The electronic absorption spectra of blue copper proteins at wavelengths longer than 400 nm are all similar. A typical spectrum is that of poplar plastocyanin, shown in Figure 1. The prominent absorption peak near 600 nm represents the cysteine sulfur to copper ($RS^- \rightarrow Cu^{2+}$) LMCT transition involving the sulfur orbital with approximate σ symmetry with respect to the Cu–S(Cys) bond.

As a group, the blue copper proteins also exhibit a number of notable similarities in their RR spectra. A typical spectrum is

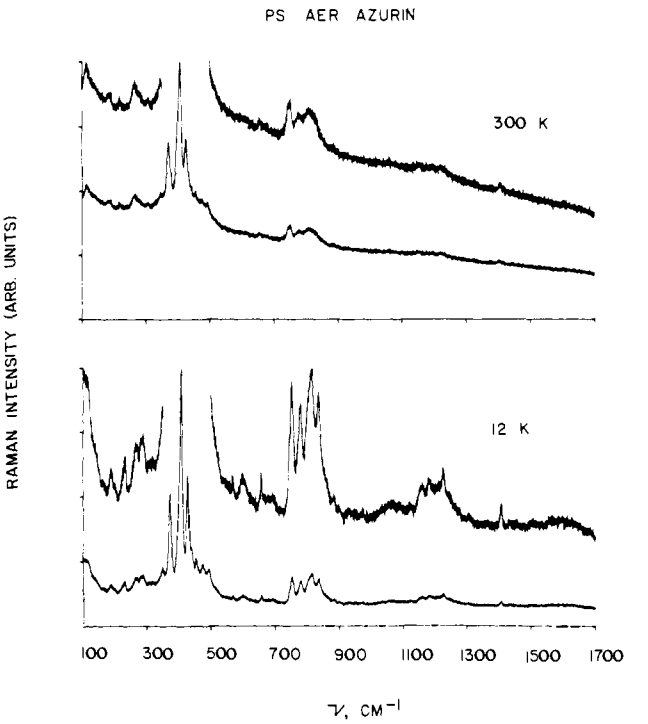

Figure 2. RR spectra of PA azurin at the temperature indicated. Laser wavelength, 647.1 nm.

that of PA azurin, shown in Figure 2 at 300 and 12 K. The most conspicuous features are the intense peaks near 400 cm^{-1}, which are resonance-enhanced by factors of ca. 10^3 compared to the normal Raman intensity of the symmetric stretch of sulfate ion. All the proteins have one or two medium intensity peaks in the 250–280-cm^{-1} region. In all cases, the RR features below 500 cm^{-1} are due to vibrational fundamentals; i.e., no fundamentals are observed which may produce overtones or combinations at the observed frequencies in this region, and difference modes cannot be a factor under the cryogenic conditions employed. By contrast, above 500 cm^{-1}, the spectra are dominated by overtones and combinations. This is particularly evident at low temperature (Figure 2), where both the relative intensity and the resolution of the overtones and combinations are enhanced. In Figure 2, three sets of peaks at ca. 800, 1200, and 1600 cm^{-1} are observed which represent the overtone/combination progressions of the fundamentals near 400 cm^{-1}. A few fundamentals appear above 500 cm^{-1}, for example, the sharp peaks in the azurin spectra at 569, 657, and 1407 cm^{-1} and the broad, incompletely resolved feature near 1500 cm^{-1} (Figure 2). The assignments of these features are discussed elsewhere.[14] For all systems examined, all the peaks exhibit polarized Raman scattering with a depolarization ratio of approximately 0.3 as expected if the scattering is dominated by a single element of the scattering tensor.

Notwithstanding the generic similarities among the RR spectra, substantial differences are observed among the different proteins and even among preparations of the same protein from different organisms. The differences include the number of vibrational modes observed and their frequencies, relative intensities, peak widths (i.e., resolution) and line shape (degree of Gaussian or Lorentzian character), overtones and combinations, isotope shifts, and the temperature dependences of all these characteristics. This diversity is evident in Figures 3–7.

The RR spectra of azurins from PP, PA, IS, BB, and AF are shown in Figure 3. The spectrum of BP azurin is omitted from this figure because of its close similarity to that of BB. The fundamental frequencies are summarized in Table I and the overtones and combinations in Table II. Table III presents the isotope shift data for the azurins studied in H_2O and D_2O and with ^{65}Cu or ^{63}Cu substituted for natural abundance copper (70% ^{63}Cu). The RR spectrum of stellacyanin (Japanese lacquer tree) is shown in Figure 4, and the frequencies and isotope shifts (^{65}Cu

(38) Reinhammar, B. *Biophys. Acta* **1970**, *205*, 35.
(39) Ferris, N. S. Ph.D. Thesis, The University of Texas at Austin, 1981.

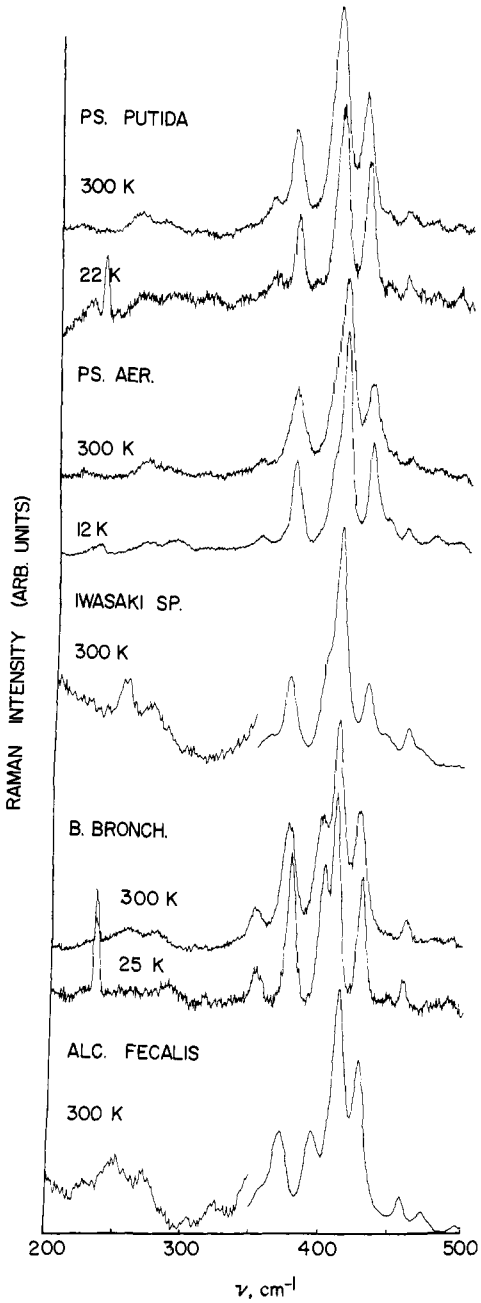

Figure 3. RR spectra of PP, PA, IS, BB, and AF azurins at the temperatures indicated. Laser wavelengths: 620 nm for IS and AF; 647.1 nm for PP, PA, and BB. The sharp feature at 233.1 cm^{-1} in PP and BB is a Kr^+ plasma emission line.

shifts from ref 20) are given in Table IV. Stellacyanin from the Chinese lacquer tree gave nearly identical results. The spectra of plastocyanins from bean and spinach are shown in Figure 5, and their frequencies are given in Table V. The spectra of (Japanese) tree and fungal laccases are shown in Figure 6. As with the stellacyanins, the laccases from Japanese and Chinese lacquer trees were very similar. Finally, the spectra of ascorbate oxidase and ceruloplasmin are shown in Figure 7. The observed RR frequencies of the multicopper oxidases (laccases, ascorbate oxidase and ceruloplasmin) are given in Table VI. In the case of tree laccase, it has been verified via wavelength dependence of the RR intensities that only the vibrations coupled to the type 1 copper chromophore are observed.

All the spectra displayed were obtained at 10–30 K except fungal laccase (77 K), IS and AF azurins (277 K), and ascorbate oxidase and ceruloplasmin (277 K). Other than minor line narrowing with cooling, no pronounced effects of temperature between 100 and 10 K were noted in any of the systems examined.

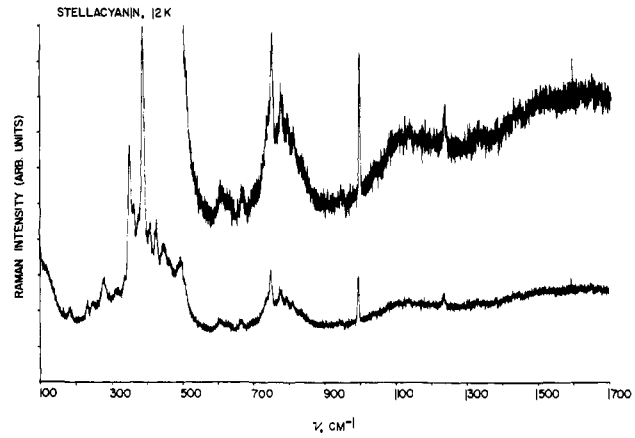

Figure 4. RR spectrum of stellacyanin at 12 K. Laser wavelength, 647.1 nm. The sharp feature at 992.4 cm^{-1} is the symmetric stretching mode of the SO_4^{2-} intensity standard.

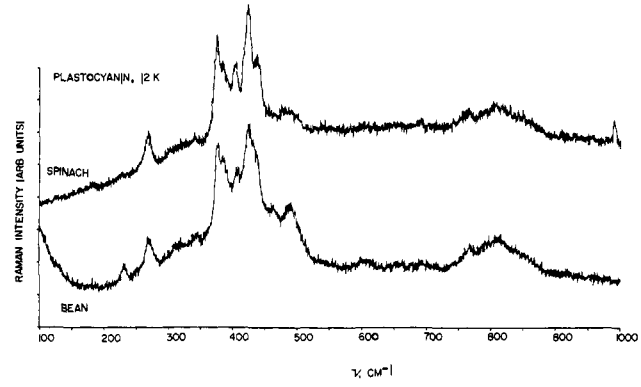

Figure 5. RR spectra of spinach and bean plastocyanins at 12 K. Laser wavelength, 604.0 nm.

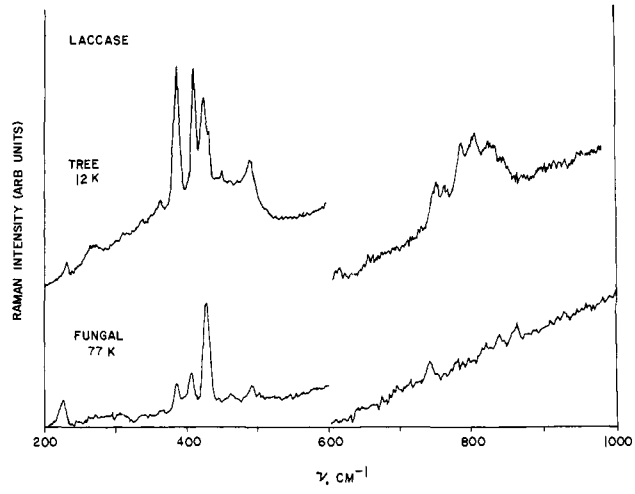

Figure 6. RR spectra of tree and fungal laccases at the temperatures indicated. The overtone regions (>600 nm) are scale-expanded by a factor of approximately 4. Laser wavelengths, 647.1 nm (tree), 620 nm (fungal).

Between 100 K and ambient temperature, however, profound temperature-dependent effects are observed in several of the proteins. Some of these have been reported previously for PA azurin and spinach plastocyanin.[14] The general effects of decreasing temperature from 300 to <100 K include dramatic suppression of background scattering, improved spectral resolution (peaks a factor of 1.5–2 narrower), frequency upshifts of ca. 2 cm^{-1} (with several significant exceptions), increases of 30–50% in the integrated intensities of overtones and combinations relative to fundamentals, and larger deuterium shifts. In specific instances to be discussed in subsequent sections, we observe peak shifts of

Table I. Azurin Fundamentals, 12 K (300 K), cm^{-1}

	PP	PA	IS	BB	BP	AF
A	113 (110)	116 (114)		114 (115)	112 (115)	
B	136 (133)	138 (140)		136	137 (136)	
C	167 (165)	165				
D	183 (183)	188 (185)		(184)	(178)	
E		199		191	192	
F	223 (213)	222 (220)		223 (225)		(225)
G	259 (258)	266.1 (263)	(252)	258 (256)	255 (255)	(251)
H	283 (275)	286.7 (278)	(271)	285 (276)	288 (277)	(272)
I	308 (304)	308 (307)		(304)		(307)
J	333 (333)	333		333 (335)		
K	356 (354)	348.2 (347)	(359)	349 (348)	350 (349)	(357)
L	372 (370)	372.6 (371.6)	(374)	374 (372)	377 (372)	(372)
M	~400	400.5 (401.6)	(399)	399 (397)	399 (398)	(394)
N	404 (402)	408.6 (408.0)	(409)	407 (408)	408 (409)	(412)
O	423 (421)	427.9 (426.7)	(429)	426 (424)	427 (424)	(426)
P	438 (437)	441 (440)	(443)	446	447	
Q	452 (452)	454.6 (456)	(458)	457 (458)	459 (457)	(456)
R	472 (472)	474 (476)	(468)	475 (480)	473	(471)
S	490 (488)	492 (489)		490 (489)	493 (492)	(497)
T	566	569		563		
U	654 (649)	657.1		659 (653)	656	
V	677 (675)	678				
W	743 (739)	753.2		754 (749)	753 (750)	
X		932				
Y		975				
I		1036				
II		1054				
III		1068			1068	
IV		1093				
V		1407				
VI		1434				
VII		1649				

Table II. Azurin Overtones and Combinations, 12 K (300K), cm^{-1}

assignment	PP	PA	BB	BP
G + N	654	668		
H + M			682	682
H + N		693		
2K			700	700
2L	~743	745	745	745
L + M			776	775
L + N	775	780.3	783	780
2M	796	802		
M + N		809	802	805
2N	806	814		
N + O	825	836.2	833	833
2O	(843)	855	854	854
N + Q	858	864.0		
N + R		883		
O + Q				
N + S		901		
L + W		1123		
2L + N		1155		
N + W		1160		
O + W		1182		
P + W		1193		
2N + M; L + N + O		1212		
3N		1226		
2N + O		1247		
N + 2O		1264		
3O		1278		
2N + S		1308		
2L + W		1499		
2N		1566		
N + O + W		1588		
3N + L		1599		
2N + L + O		1612		
4N		1627		

5–15 cm^{-1}, relative intensity changes among fundamentals, and discontinuous line-width changes.

Table III. Azurin Isotope Shifts, 25 K (300K), cm^{-1}, Deuterium Shift [^2H–^1H]/Copper Shift [^{65}Cu–^{63}Cu]

peak, ν (PA azurin)	isotope shifts		
	PA	IS	AF
G, 266.1	0/~+1		
H, 286.7	−5/~0		
K, 348.2	−2/~0		
L, 372.6	−0.9 (−0.3)/−0.6 (−0.7)	(−0.4)/(−1.0)	(−0.7)/(−1.4)
M, 400.5	---/−0.6 (−1)	---/(−0.3)	---/(−0.3)
N, 408.6	−1.0 (−0.3)/−0.6(−0.8)	(−0.2)/(−1.0)	(−0.4)/(−1.6)
O, 427.9	−1.2 (−1.4)/−0.2 (0.0)	(−1.4)/(−0.2)	(−1.5)/(−0.3)
P, 441	−1.5		
Q, 454.6	0.0 (−0.6)/~0	(−1.0)/(~0)	(−1.3)/(---)
R, 474	−1.0/~0 (~0)	(−1.9)	(−2.1)/(~0)
S, 492	+1.3/~0 (~0)		
T, 569	−2		
U, 657.1	+0.3		
W, 753.2	0.0		
L + N, 780.3	−2.4		
2N, 814	−2.1		
N + O, 836.2	−1.7		

Table IV. Stellacyanin Frequencies and Isotope Shifts, 12 K (300 K), cm^{-1}

	ν	D shift, ^2H–^1H	Cu shift,[a] ^{65}Cu–^{63}Cu
	Fundamentals		
A	117 ± 1 (108)		
B	183 ± 1 (174)		
C	248 ± 1 (249)		
D	276.2 ± 0.5 (272)	−2.9, −2*	(~0)
E	335.1 ± 0.4		
F	348.7 ± 0.4 (348)	−1.8 (~0)	(−1.8)[a]
G	361.0 ± 0.6 (358)	−2[a] (−2–3)[a]	(−2–3)[a]
H	374.2 ± 0.8 (373)	−3[a]–4(−2–3)[a]	(−2–3)[a]
I	386.7 ± 0.3 (387)	−2.3 (−0.6)[a]	(−1.5)[a]
J	399 ± 1 (399)		
K	406.7 ± 0.3 (408)	−1.4	
L	424.3 ± 0.5 (423)	−1.8	
M	445.6 ± 0.8 (446)	−2	
N	463 ± 1 (465)		
O	493 ± 1 (495)		
P	747 ± 1 (746)	−1.7	
Q	941		
I	1033		
II	1103		
III	1194		
IV	1233 (1230)		
V	326		
VI	1430		
VII	1502		
VIII	1621		
IX	1644 (1639)		
X	1672		
	Overtones and Combinations		
D + F	625 (626)		
D + I	663		
2F	699		
F + I	735 (732)	−4.0	
2I	775 (777)	−4.3	
I + K	793	−6	
I + L	810		
I + M	830		
I + N	848		
2F + I	1080		
I + P	1134		
4F	1379		
2F + P	1443		

[a] Data from L. P. Nestor et al. (ref 20), 77 K (300 K).

RR excitation profiles at 10 K have been determined for PA azurin, spinach plastocyanin, and stellacyanin. Laser wavelengths used include Kr^+ laser lines at 568.2, 647.1, and (for azurin) 674.6 nm and tunable dye laser lines at 587, 604, 607, and 627 nm. Qualitative RR intensity data have been obtained for tree laccase

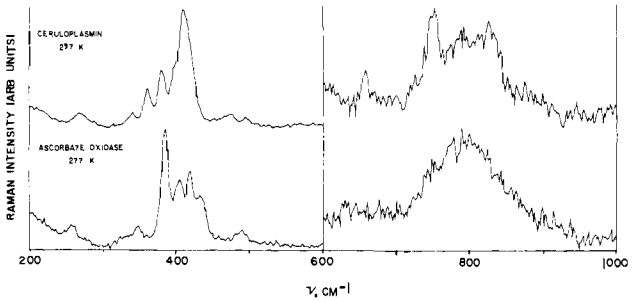

Figure 7. RR spectra of human ceruloplasmin and zucchini squash ascorbate oxidase at 277 K. The overtone regions (>600 nm) are scale-expanded by a factor of approximately 5. Laser wavelength, 620 nm.

Table V. Plastocyanin Fundamentals, 12 K (300 K), cm^{-1}

	spinach	bean	poplar[a]
A	183		
B	270.1 (267)	272 (266)	270
C	302		
D	328 (331)	323	
E	343.1 (342)	344	
F	377.3 (376)	378 (376)	376
G	387	387 (384)	385
H	393	394	392
I	406.5 (403)	408 (405)	407
J	425.3 (423)	427 (425)	423
K	441.5	440 (432)	439
L	480 (478)	464	
M	491 (492)	492	
N	767 (753)	769 (762)	765
O	950		
P	1040	1049	
Q	1080	1060	
R	1095	1080	
	Overtones and Combinations		
B + G	645		
B + H	654	656	
B + K	694	695	
B + L	710	716	
G + J	786	791	
unresolved	810	810	
J + L	849	850	
K + L	866		
2G + K	1180		
unresolved	1210	1210	
2K + G	1223	1227	
2K + H	1244		
2K + J	1252	1255	

[a] Preliminary results; J. R. Schoonover, W. H. Woodruff, O. Farver, and I. Pecht.

at 568.2, 604, 647.1 nm. Despite the better peak resolution and signal-to-noise at 10 K and the concomitantly more accurate and precise peak areas, neither vibronic structure nor significant changes in relative peak intensities due to selective RR enhancement are observed in the profiles of either the prominent or the weak peaks. The RR intensities all reach their maximum at approximately the same wavelength as the electronic absorption maximum, as expected for a simple Franck–Condon resonance mechanism involving only the Cu^{2+}–S(σ)(Cys) ligand-to-metal charge-transfer (LMCT) chromophore.

Discussion

Resonance Raman Intensities. A central issue in understanding RR spectra is valid interpretation of the intensities. The RR intensity data are unique in that they illuminate the interplay of the vibrational and electronic states of the molecule in question. Given reliable variational assignments, RR intensity arguments can be useful in assigning electronic transitions and, conversely, vibrational assignments can be strengthened if the nature of the resonant electronic transition is known. The RR intensities and other vibrational information such as frequencies, line shapes, isotope shifts, temperature dependences, etc., comprise the data set from which structural and dynamical information may be inferred.

Table VI. Oxidase Fundamentals, 12 K (277 K), cm^{-1}

	tree laccase	fungal laccase	ascorbate oxidase	cerulo-plasmin
A	101			
B	121			
C	180			
D	203			
E	265 ± 2 (263)	268 (268)	(258)	(268)
F	275 ± 2			
G	337 ± 2			
H	348 (344)	345 (336)	(346)	(340)
I	362.9 ± 0.7 (361)	366 (366)		(361)
J	382.8 ± 0.5 (379)	386 (386)	(385)	(380)
K	391			
L	405.9 ± 0.5 (404)	406 (408)	(405)	(412)
M	420 ± 1 (419)		(421)	
N	428.4 ± 0.9	428 (428)	(432)	
O	447.3 ± 0.7 (446)			
P	459	462 (464)		
Q	472			(472)
R	489.8 ± 0.7 (491)	490 (492)	(488)	(492)
S	571			
T	614			
U				(657)
V	731			
W	753 (747)	742 (740)	(744)	(750)
X	951			
I	1044			
II	1076			
III	1143			
IV	1171			
V	1223			
VI	1279			
VII	1451			
VIII	1674			
	Overtones and Combinations			
I + J	747			
2J	766 ± 1		(772)	
J + L	788 ± 2 (786)			(792)
unresolved			(798, br)	
2L	806.9 ± 0.8 (807)			(828)
J + N		818		
L + M	829 ± 2 (830)	833		
M + N	848 ± 5			
2N		862		
J + R	874			
L + R	896			

Previously, most experimentalists have interpreted RR intensities by using theoretical treatments based on the Kramers–Heisenberg–Dirac expression (KHD), for example,

$$I_{10}{}^{k}(\nu_{\text{laser}}) = (\text{constants})\cdot\sum_{n}\left|\epsilon_{00}\,\frac{\langle g_1|e_n\rangle\langle e_n|g_0\rangle}{\nu_{eg}-\nu_{\text{laser}}+i\Gamma}\right|^2 \qquad (1)$$

where ϵ_{00} is the pure electronic extinction coefficient, g_0 and g_1 are vibrational wave functions of normal mode k in the ground electronic state, e_n is a specific vibronic level in the electronically excited state, ν_{eg} is the transition frequency between g_0 and e_n, ν_{laser} is the laser frequency, and $I_{01}{}^{k}$ is the RR intensity of the fundamental of vibrational mode k. Equation 1 indicates that RR intensities (i) increase with the square of ϵ_{00}, (ii) increase as the frequency of the laser light approaches the frequency of the resonant electronic transitions, and (iii) are related to the magnitudes of Franck–Condon factors $\langle e_n|g_m\rangle^2$. Point (iii) leads to the expectation that a given normal vibrational mode will be resonance-enhanced to the extent that the equilibrium nuclear positions of the resonant excited state are displaced from their ground-state positions along the normal coordinate in question. In the case of blue copper proteins, the resonant transition is the RS^{-}(Cys) → Cu^{2+} LMCT, and the resonant excited state may be described approximately as RS·(Cys)–Cu^{+}. Resonance enhancement is thus expected only for those normal modes whose

coordinates are affected by this transition.

An alternative theoretical description of the RR process has recently been developed by Heller and Tannor.[23,24] This approach examines the temporal evolution of the scattering process in terms of wave-packet dynamics. One attractive feature of this approach is that it provides a practical guide for the interpretation of RR intensities which is more readily visualized than that furnished by the KHD approach. The two approaches are the same in principle, simply related by the Fourier transform: Heller–Tannor theory examines the RR scattering process in the time domain, in contrast to the KHD approach which does this in the frequency domain. However, it is explicitly clear in the time-domain approach that there is no need to consider the multitude of eigenstates of the excited electronic state or the associated Franck–Condon factors, as the summation in the KHD formulation implies (eq 1). This is because the RR scattering process occurs on a time scale which is short compared to the period of molecular vibrations, and therefore there is insufficient time for the vibronic eigenstates to be resolved. In this view, RR intensity is the result of the *classical* force V_k' exerted by the excited-state potential surface at the equilibrium nuclear coordinates of the ground state (Franck–Condon (FC) point). The RR intensities are shown to be a consequence of these forces acting on the initial ground-state vibrational wave function g_0 when it is transported by the incident laser photon to the excited-state potential surface and temporally evolved as $g_0(t)$ before returning to the final state (described by g_1) by the scattering of the photon (ref 23 and 24 and references therein). The counterpart of eq 1 in this formulation is

$$I_{01}{}^{k}(\nu_{\text{laser}}) = (\text{constants}) \cdot \int_0^\infty |e^{i(\nu_{\text{laser}})t-\Gamma t}\epsilon_{00}\langle g_1|g_0(t)\rangle\, dt|^2 \qquad (2)$$

Equation 2 leads to the following useful predictions for the interpretation of RR intensities: (i) since $\langle g_1|g_0\rangle \equiv 0$, RR intensities are nonzero only to the extent that g_0 evolves with time in response to the force imposed by the excited-state potential surface, i.e., to the extent that $\langle g_1|g_0(t)\rangle \neq 0$; (ii) for any ground-state vibrational mode k, the RR intensity will be proportional to the square of the projection upon k of the first derivative of the excited-state potential ($dV/dq_k = V_k'$), evaluated at the FC point, i.e., to the square of the classical force along k due to the excited-state potential in the FC region. The specific expression relating RR intensities for any two normal modes k and l to the excited-state forces along the two coordinates is[24]

$$(I_{01}{}^{k}/I_{01}{}^{l}) = (\nu_l/\nu_k)[V_k'/V_l']^2 \qquad (3)$$

The relative intensities of the various modes are seen to be related to the steepness of the upper potential surface in the FC region. If the excited-state potential is harmonic and other simplifying assumptions[24] are valid, eq 3 yields relative excited-state coordinate displacements Δ, e.g.,

$$(I_{01}{}^{k}/I_{01}{}^{l}) = (\nu_k{}^3\Delta_k{}^2/\nu_l{}^3\Delta_l{}^2) \qquad (4)$$

Expressions similar to eq 3 and 4 give relationships among overtone and combination intensities. It is significant to note that RR fundamentals can only have nonzero intensity if $V_k' \neq 0$. Overtones, on the other hand, may have nonzero intensity if $V_k' \neq 0$ *or* if the second derivative V_{kk}'' differs from that of the ground state (viz., if the force constant of mode k changes upon electronic excitation). Combinations between modes k and l may have nonzero intensity if *both* $V_k' \neq 0$ *and* $V_l' \neq 0$ *or* if $V_{kl}'' \neq 0$ (the nonzero second derivative requires the excited-state normal modes to differ from those of the ground state, that is, requires Duschinsky rotation to occur).[24,25] Finally, we note that displacement of nuclear coordinates in the excited state is necessary, as the KHD intuition suggests, but not sufficient for significant RR enhancement of fundamentals. A mode which has a shallow excited-state potential may experience large displacement but still have small RR intensity if V' is small.

Vibrational Assignments: Azurin. Crystallographic determination of the structures of two azurins[7,8] shows that the azurin active site is quite similar to that of plastocyanin (Figure 1). The azurin structures are less precise than that of poplar plastocyanin but there may be significant differences in the Cu–S(Met) bond distance and the conformation of the copper-bound methionine residue in azurin compared to plastocyanin.[6-8] The azurin fundamental frequencies at 300 and ca. 12 K are given in Table I. Overtone and combination frequencies at 300 and ca. 12 K are collected in Table II. Fundamentals below 1000 cm^{-1} are assigned letters (A–W) and those above 1000 cm^{-1} are designated by Roman numerals.

(a) Peaks G and H (ca. 270 cm^{-1}). We previously proposed assignment of these modes as predominantly Cu–N(His) stretch.[14,18,22] This assignment is supported for peak H (287 cm^{-1} at 12 K) by our isotopic substitution data (Table III). A large deuterium shift (5 cm^{-1}) is observed under conditions in which all labile protons including the N-3 and C-2 protons of His–Im have been substituted. This is consistent with designation of peak H as the symmetric Im–Cu–Im stretch, which involves much imidazole motion and therefore is sensitive to mass changes involving imidazole. In this symmetric stretch, the displacement of the copper atom is minimized; therefore, the copper isotope shift is expected to be minimal. We observe the copper isotope shift to be zero within experimental error (which we estimate to be ± 0.5 cm^{-1} for these weak peaks). Our analysis of the azurin isotope data for peak H leads to conclusions similar to those reached by other workers[20] for the analogous mode in stellacyanin.

The temperature dependence of the RR intensities of peaks G and H suggests that they are coupled modes (vide infra). Nevertheless, the isotope data suggest that peak G is a mode which contains little Cu–N stretching character. The deuterium isotope shift is zero, and the ^{65}Cu shift is, in fact, slightly *positive*. Thus, peak G cannot be a motion involving displacement of groups containing labile protons (e.g., His–Im) nor can it involve significant displacement of the copper atom. Motions which might be near 270 cm^{-1} and couple to the Cu–N stretch include the Cu–S(Met) stretch, the Cu–S(Cys)–C_β(Cys) angle bend, and the methionine C–S–C angle bend. The first two of these must exhibit a substantial negative ^{65}Cu isotope shift, which peak G does not. Our data are consistent with assignment of peak G as the methionine C–S–C angle bend, but this assignment appears to be excluded by selenomethionine-substituted azurin data obtained by other workers.[19] The assignment of this mode remains obscure, but we note that plastocyanin (which has very weak or nonexistent Cu–S(Met) bonding[6,14]) and stellacyanin, which lacks methionine, do not exhibit the temperature-dependent splitting of the feature near 270 cm^{-1} as does azurin, which has been proposed to have significant Cu–S(Met) bonding.[14]

Concerning the isotope shifts in peak H, we note that the magnitude of the deuterium shifts is not consistent with a point mass model for the ligands in the CuN_2SS^* site. In such a model, the maximum deuterium shift expected for the in-phase stretch, which occurs at θ(NCuN) = 180°, is 4 cm^{-1} for a change in the imidazole mass of 2 amu. This extreme geometry is inconsistent with the crystal structure. Vibrational model calculations by others,[20] based on point masses for the imidazoles and θ(NCuN) = 97°, predicted deuterium isotope shifts of ~ 2 cm^{-1} for the in-phase mode. However, coupling of the Cu–N stretches to internal ligand deformation modes may well be important and most likely accounts for the large ^2H isotope shift and the dependence of peaks G and H upon temperature and species to be discussed below.

(b) Bands Near 400 cm^{-1}. The only Cu–L stretching vibration expected near 400 cm^{-1} is the Cu–S(Cys) stretch.[14,18] This view has recently been strengthened by isotope studies on stellacyanin.[20] As in the stellacyanin study, our azurin $^{65}Cu/^{63}Cu$ isotope shifts (Table III) show that no single peak near 400 cm^{-1} is accurately described as pure Cu–S stretch. The ^{65}Cu shift of such a mode, if unmixed, should be approximately −3 cm^{-1}.[20] None of the strong peaks near 400 cm^{-1} show a ^{65}Cu shift larger than −1.5 cm^{-1}. The aggregate ^{65}Cu shift of peaks L, M, N, and O is approximately 3 cm^{-1} for all the azurins examined, and the ^{65}Cu shifts of all the other peaks above 200 cm^{-1} (except peak G) are approximately zero.

For all three azurins studied by Cu isotope substitution, a close correlation was found between the relative peak intensities near 400 cm^{-1} and the frequency separation from the intense, ca. 405 cm^{-1} peak (peak N). Upon ^{65}Cu substitution, the modes at lower frequency than the intense peak gain intensity relative to those at higher frequency. This suggests that the Cu–S(Cys) stretching potential is distributed primarily among peaks L, M. N, and O and that the fractional Cu–S character of these modes is the most important source of RR intensity for all these peaks. This observation is important in determining the natural frequency of the Cu–S stretch as a local oscillator (vide infra).

It is clear from the isotope shifts and isotope-sensitive intensities that modes L, M, N, and O all contain significant contributions from that Cu–S stretch. Four normal modes are observed, however, and at least four internal coordinates must contribute to them. Three of these must be internal deformation coordinates of the ligands because the other Cu–L stretches are at much lower frequency.

One ligand coordinate that is structurally forced[6,8] to couple to the Cu–S stretch is the cysteine $S–C_\beta–C_\alpha$ angle bend. The copper atom, S, C_β, and C_α are all nearly coplanar (in plastocyanin, the dihedral angle $(Cu–S–C_\beta)$, $(S–C_\beta–C_\alpha)$, is 170°; in azurin, it is close to this value, although its precise specification will require further refinement of the crystal structure). The frequencies of the cysteine stretching fundamentals ($\nu(C_\beta–S)$ = 753 cm^{-1}, $\nu(C_\alpha–C_\beta)$ = 975 cm^{-1}) suggest that the natural frequency of the $C_\alpha–C_\beta–S$ angle bend is near 400 cm^{-1}. This fact and the temperature dependence of the relative intensities of peaks M and N led us to assign these modes as predominantly due to the coupled Cu–S stretch and $S–C_\beta–C_\alpha$ angle bend. The isotope shifts are consistent with this assignment if peak N is the in-phase mode. In this mode, the Cu–S distance increases as the $S–C_\beta–C_\alpha$ angle becomes larger, which results in a large displacement of the copper atom and hence a large copper isotope effect (Table III). The out-of-phase mode M would involve a large displacement of the sulfur atom, and a smaller ^{65}Cu shift is expected (AF azurin, Table III). The coupling of the Cu–S stretch and the $S–C_\beta–C_\alpha$ angle bend is strongly dependent upon two angles: the dihedral angle $(Cu–S–C_\beta)$, $(S–C_\beta–C_\alpha)$, as has been noted by others,[20] and the $Cu–S–C_\beta$ angle. Maximum coupling occurs if the dihedral angle is 180° (all atoms coplanar) and the $Cu–S–C_\beta$ angle is approximately 150°. We will return to this point below in our discussion of the temperature dependence of the azurin RR spectrum.

Modes L and O are also mixed modes involving the Cu–S stretch and internal ligand coordinates. The identity of the contributing ligand coordinates cannot be established from the present data. Two possibilities are evident: the ligand motions may be deformations about the cysteine α-carbon atom or they may be deformations of the His–Im structures. Some of us have previously suggested the latter interpretation.[14,18] The deuterium shifts of these modes clearly require the involvement of a group having labile protons, but it can be argued that this is the cysteine amide NH. Indeed, both cysteine and histidine motions may be involved. Selective isotope substitution using microbiological techniques appears to be the only way to settle this issue satisfactorily.

(c) Overtones and Combinations. The RR intensities of the overtone and combination bands near 800 cm^{-1} give additional clues as to the identity of the peaks containing large contributions from the Cu–S stretch. From eq 3, we note that the relative RR intensities of vibrational fundamentals scale as the square of the first derivative of the excited-state potential surface, V_k', evaluated at the ground-state equilibrium nuclear position.

Overtones and combinations may gain intensity from V_k' effects as well. Via this mechanism, overtones obtain intensity which scales as $(V_k')^4$, and combination $(\nu_k + \nu_l)$ bands obtain intensity which scales as $2(V_k')^2(V_l)^2$.[24] Therefore, if overtones and combinations derive their intensities only from first-derivative mechanisms, relative overtone intensities should be equal to the relative fundamental intensities squared (eq 3), and the combinations of a series of fundamentals x with a given fundamental k should have relative intensities $I(\nu_k + \nu_x)$ simply equal to twice the relative intensities of the fundamentals $I(\nu_x)$. Both overtones and combinations, however, may gain RR intensity from second-derivative effects as well as from V' effects. In the case of overtones, this effect scales as the square of the force constant change between the ground and excited states, namely $(F_k - V_{kk}'')^2$, where F_k is the ground-state force constant. For combinations, the second-derivative intensity scales as $(V_{kl}'')^2$. If *both* V' and V'' effects contribute significantly to overtone or combination intensities, the first- and second-derivative contributions are approximately additive when on-resonance excitation is employed.[24,25,40] We note that enhancement of combinations by second-derivative effects requires $V_{kl}'' \neq 0$, which in turn requires the ground-state normal modes k and l to be mixed in the excited state or, in other words, requires Duschinsky mixing. Finally, overtones and combinations are subject to deenhancement by multimode effects which exert a $1/\sigma^4$ decrement (where σ is the multimode parameter) upon fundamental and second-derivative overtone and combination intensities but are more severe $(1/\sigma^6)$ for first-derivative overtone and combination intensities.[24]

Table VII. Relative Intensities[a] of Overtone and Combination Peaks in Azurin

peak	I (obsd)	I (pred)[b]
2L	0.19	0.27
L + N	1.00	1.00
2M	0.58	0.27
M + N	0.25	1.01
2N	1.20	0.93
N + O	1.19	1.10
2O	0.23	0.30
N + Q	0.16	0.16
N + R	0.17	0.16

[a] Relative to L + N combination peak = 1.00. [b] Predicted values from Heller theory (see text). Relevant equations: $(I_{10}^k/I_{01}^l)^2 = I_{02}^k/I_{02}^l$; $I_{01}^x/I_{01}^y = 2(I_{k+x}/I_{k+y})$ for fundamental peaks k, l, x, and y, the corresponding overtones and the combinations $k + x$ and $k + y$. Relative intensities of the fundamental peaks are given in Table IX.

Simple analytical expressions can be derived[24,25,40] which relate the relative intensities of fundamentals, overtones, and combinations. Table VII gives the observed peak areas of the overtones and combinations in PA azurin, relative to the area of the isolated combination peak L + N = 1.00. The relative intensities of the overtones and combinations predicted assuming only V_k' enhancement are also given in Table VII. It is seen that the observed relative intensities are in reasonable agreement with the predictions except that the overtones 2M and 2N are somewhat more intense than predicted and the combination M + N is substantially weaker than predicted. The aggregate intensity of all three of these peaks is, however, in satisfactory agreement with the predicted aggregate intensity. The enhanced intensity of the overtones is readily interpreted in terms of the change in force constant $(F_k - V_{kk}'')$ expected for the modes containing large contributions from the C–S stretch, because this force constant should experience a larger change between the $Cu^{2+}–SR^-$ ground state and the $Cu^+–SR(\cdot)$ excited state than that of any other coordinates. The implication of the *overtone* intensities is therefore that the *fundamentals* M and N contain more Cu–S stretch in their potential energy distributions than the other modes. The fact that all observed combinations involve mode N may suggest that the large change in the Cu–S force constant in the excited state results in significant Duchinsky effect for modes involving the Cu–S stretch, therefore, in V_{NX}'' (for combination N + X) becoming substantially nonzero. The reason for the diminished intensity of combination M + N is not entirely clear, but it may be that the nearly planar constraint on the Cu–S–C–C structure prevents significant Duschinsky mixing of modes M and N.

Azurin Variation with Organism and Temperature. Although the RR spectra of azurins from different bacteria are similar with regard to the number and the relative intensities of peaks observed, there exist substantial differences in detail. In Figure 3, the various azurin spectra are arranged in order of the progression of the most

(40) Morris, D. E.; Woodruff, W. M. *J. Phys. Chem.*, submitted.

obvious of the changes, namely in peaks G and H (see Table I) near 270 cm^{-1} and in peaks M and N near 400 cm^{-1}. Generally speaking, as one progresses through this series from top to bottom, the following changes occur progressively: (i) the splitting between peaks G and H increases; (ii) peak H becomes relatively more intense than peak G; and (iii) peaks M and N become progressively better resolved as peak M shifts monotonically to lower frequency and peak N to higher frequency. The progressive changes in the RR spectra are apparently due to progressive structural differences in the blue copper sites of the various proteins.

The spectral changes observed in PA azurin as a function of temperature to some extent mimic the changes noted among the various azurins at constant temperature: with decreasing temperature, (i) the frequency difference between peaks G and H increases; (ii) peak H increases in intensity relative to G; and (iii) the resolution of peaks M and N improve (Figures 2 and 3, Table I). These observations may be helpful in understanding the structural basis for the observed spectral variations among the various azurins. Vibrational effects which are observed in a series of proteins with different features, such as primary structure, may be interpreted with a greater degree of confidence if they also occur in a given protein as a function of temperature. Thus, conclusions concerning the temperature dependence of the spectra for a given azurin may illuminate the structural differences among the azurins. Toward this end, we proceed now to discuss the temperature data for PA azurin, the one that we have studied in the greatest detail. (In every case where comparisons have been made, the PA results are analogous to those on the other azurins.)

On the basis of our isotope substitution experiments, we have assigned peak H as predominantly the symmetric Cu-N(His) stretch. We noted that neither the ^2H nor the ^{65}Cu shifts in peak G support its assignment as a Cu-N stretch, although the precision of the isotope shifts is limited because of the low intensity of these peaks. The temperature-dependent data suggest that peaks G and H are nevertheless coupled modes and that their coupling is temperature-dependent. The total integrated intensity of peaks G and H relative to the integrated intensity of all the RR peaks between 200 and 500 cm^{-1} is independent of temperature. However, the integrated intensity of G relative to H diminishes by a factor of 2.5 between 300 and 10 K. The temperature dependence of the relative intensities of bands G and H may be ascribed to a change in the ground-state PEDs of these modes, which would involve a temperature dependence of geometrical factors or a change in the character of the excited-state distortion which makes it more or less symmetric with respect to the coupled oscillators. The larger-than-predicted ^2H shift in peak H may support the former explanation. Because the identity of the motion(s) comprising peak G is uncertain at this time, the structural rationale for the temperature-dependent coupling is also uncertain.

Similar temperature-induced frequency shifts and relative intensity changes are observed for peaks M and N near 400 cm^{-1}. In PA azurin, the area of peak N increases by a factor of 1.4 relative to peak M as the temperature is lowered from 300 to 12 K, even though the integrated area of peaks M plus N relative to the integrated area of all peaks between 200 and 500 cm^{-1} remains nearly constant. The splitting between peaks M and N is approximately 2 cm^{-1} greater at 12 K than at 300 K. These observations are consistent with a stronger coupling of the contributing oscillators at lower temperature. Since the (Cu-S-C_β)-(S-C_β-C_α) dihedral angle is already near its optimum value for coupling at room temperature, this suggests that the Cu-S-C_β angle is the primary determinant of the coupling between the Cu-S(cys) stretch and the S-C_β-C_α bend. Thus, the data suggest that the primary temperature-induced structural change involving the copper–cysteine unit in PA azurin is an increase in the Cu-S-C_β angle, which may reflect a displacement of the Cu atom into the N_2S(Cys) plane, possibly due to apical constraint by S(Met) at low temperature.

It is clear that the RR spectra, in contrast to EPR and electronic spectra, are sensitive to structural features beyond the first coordination shell of the blue copper site. It is on this basis that we can understand the variations in the RR spectra of blue copper proteins with species and temperature.

Stellacyanin. Stellacyanin is notable in that it lacks methionine, has its intense RR features at lower frequency than other blue copper proteins, and exhibits other pecularities in its charge-transfer, ligand-field, and EPR spectra.[2-5] Nestor et al. have quite recently reanalyzed the RR spectrum of stellacyanin in an investigation including isotope and temperature studies.[20] The qualitative conclusions regarding vibrational assignments in the 270- and 400-cm^{-1} regions were similar to those discussed above and elsewhere[14,18,21] for azurin, plastocyanin, and oxidases, namely that ligand deformations contribute to several of the modes near 400 cm^{-1}, no single mode is accurately described as a pure Cu-S(Cys) stretch, and the Cu-N(His-Im) stretches are observed near 270 cm^{-1}.

A wide range of evidence[4,5,11,26,28] demonstrates that stellacyanin shares three ligands in common with all other well-characterized blue copper proteins, namely, two histidine imidazoles and a cysteine mercaptide. Neither the identity of the remaining ligand(s) nor the coordination number of copper is known, but four[5] and five[16] coordination have been postulated. Disulfide[17] peptide,[15] and other possibilities have been suggested as the other ligands. Nevertheless, the RR modes of the Cu$(His)_2$(Cys) core are expected to dominate the 300–500-cm^{-1} region as they do in azurin and plastocyanin, and the local oscillators which contribute to these modes are similar in all three cases. As in azurin, the manner in which the local oscillators couple to produce the observed normal modes will depend in a sensitive way upon the structure of the chromophore.

It has been argued elsewhere[20] that the natural frequency of the Cu-S(Cys) stretch in stellacyanin should be lower than in azurin or plastocyanin because the Cu-S(Cys) bond distance is longer.[11] This suggestion is supported by the observation that the intense peaks in stellacyanin occur at lower frequency than in azurin or plastocyanin (compare Figures 2, 4, and 5). Calculations using the experimentally determined Cu-S(Cys) distances of stellacyanin and plastocyanin[6-8,11] suggest that the natural frequency of the Cu-S(Cys) stretch occurs at approximately 20 cm^{-1} lower energy in stellacyanin; therefore, we expect this coordinate to distribute itself and its intensity among correspondingly lower energy normal modes.

Stellacyanin, unlike azurin, has only one prominent peak near 270 cm^{-1}, peak D (276 cm^{-1}). This may be because of the involvement in azurin of methionine modes near this frequency and the absence of methionine in stellacyanin. We observe no asymmetry in peak D which might indicate more than one contribution to the envelope. Although the feature is rather broad, it is no more so than peaks G or H in azurin or the corresponding feature in plastocyanin. The deuterium shift (Table IV) is in essential agreement with the previously reported value,[20] approximately as expected for the symmetric Cu-N(His-Im) stretch in the point-mass model,[20] and is substantially smaller than that of peak H in azurin.

It is possible that peak C in stellacyanin (248 cm^{-1}) represents the asymmetric Cu-N(His-Im) mode. This mode has no obvious counterpart in the other blue copper spectra, except perhaps peak G in azurin. Like peak G, it shows no deuterium-isotope shift. Due to poor signal-to-noise ratio at room temperature, it is not possible to tell whether intensity swapping as a function of temperature occurs between peaks C and D, as it does between peaks G and H in azurin. If peak G is the asymmetric Cu-N stretch, its ^{65}Cu shift should be significant.

Aside from the intensity distribution, which simply reflects the revised distribution of the Cu-S(Cys) stretching potential, there are no striking features below 500 cm^{-1} in the stellacyanin spectrum which offer any clues as to the identity of the fourth (or fifth) ligand, although a possible alternate assignment of the 248-cm^{-1} feature is as the Cu-S(disulfide) stretch.[41] The stellacyanin spectrum does have more peaks in the 300–500-cm^{-1}

(41) Ferris, N. S.; Woodruff, W. H.; Jones, T. E.; Rorabacher, D. B.; Ochryomowycz, L. A. *J. Am. Chem. Soc.* **1978**, *100*, 5939.

Table VIII. Relative Intensities[a] of Overtones and Combination Peaks in Stellacyanin

peak	I (obsd)	I (pred)[b]
2F	~0.2	0.37
F + I	1.00	1.00
2I	1.35	1.82
I + K	0.52	0.49
I + L	0.41	0.38
I + M	0.29	0.36

[a] Relative to F + I combination peak = 1.00. [b] See Table VII.

range than any of the other proteins, and one of these might be the stretching motion of a disulfide S–S bond somewhat weakened by coordination to copper.

In the high-frequency region, a prominent feature is observed at 1233 cm^{-1} (peak IV), and this disappears entirely upon deuteration of the labile protons in stellacyanin. This peak is definitely resonance-enhanced as its intensity as a function of laser wavelength shows. It is much more prominent at low than at ambient temperature, apparently because it is considerably broadened in fluid solution. This peak has been observed previously,[15] but its existence has been the object of some controversy.[20] Apparently, its observation depends in a sensitive manner upon solvent conditions and/or protein conformation. In any case, the obvious assignment of peak IV based upon its frequency and its behavior upon deuteration is as the amide III vibration of a protonated peptide group. Resonance enhancement of a peptide mode could occur because a backbone peptide carbonyl group is coordinated to copper or because the amide III mode of the coordinated cysteine is coupled to the charge-transfer chromophore.

The overtone and combination intensities in stellacyanin are consistent with the correlation of peak I in stellacyanin and peak N in azurin as analogous normal modes, viz. the in-phase mode derived from the Cu–S stretch and the S–C–C angle bend. Except for the feature at 625 cm^{-1} (D + F combination), all the combinations involve peak I, just as all the PA azurin combinations involve peak N. The relative intensities of the overtones and combinations in stellacyanin are given in Table VIII. The combination intensities are all self-consistent as predicted by theory;[24,25] that is, they have the same relative intensities as the fundamentals. The overtones, however, are somewhat weaker relative to the combination than predicted. Apparently multimode effects are more effective in deenhancing overtones relative to combination in stellacyanin compared to azurin, or there is more Duschinsky mixing. The trend toward "disappearing overtones"[24] while combinations persist (and indeed become more prolific) continues and becomes more pronounced in plastocyanin (vide infra).

Plastocyanin. Due to the elegant crystallographic studies of Freeman and co-workers[6] and subsequent EXAFS investigations,[9] the structure of crystalline plastocyanin at room temperature is far better known than that of any other copper protein. Previous comparative RR studies of plastocyanin and azurin[14] show that while the X-ray structures are similar, by the RR criterion considerable differences exist between the structures of the chromophores of the two proteins. Our conclusions concerning the identity of the RR modes in plastocyanin are qualitatively the same as for azurin and stellacyanin. The distribution of RR intensity as a function of peak position (Table IX) suggests a natural stretching frequency of the Cu–S(Cys) bond which is virtually the same as for azurin. The symmetric Cu–N(His) stretch is assigned as peak B (270 cm^{-1}). In plastocyanin, there is no hint of a weak feature near 270 cm^{-1} or even an asymmetry of peak B which might be attributed to the out-of-phase component of the coupled Cu–N stretches or other coupled motions. No isotope studies have yet been performed on plastocyanin, so mode correlations of the peaks of plastocyanin with azurin and stellacyanin are uncertain. However, the relative intensities (Table IX) suggest that peak J in plastocyanin (425 cm^{-1}) is correlated with peak N in azurin and peak I in stellacyanin.

The structure of plastocyanin undergoes a significant alteration at a temperature close to the freezing point of water. This temperature-dependent structural change, which is found in no other single-copper protein, probably involves an alteration of the $(Cu–S–C_\beta)–(S–C_\beta–C_\alpha)$ dihedral angle in the Cu–S(Cys) unit.[14] This accounts for the observed shift in the C_β–S(Cys) stretching frequency (Table V). At the same temperature, dramatically narrowed peak widths compared to fluid solution are observed.[14] This was attributed to vibrational-dephasing phenomena which are facile in fluid solution but are inhibited at temperatures below that of the structure change. A reasonable explanation for this change in vibrational dynamics is the formation of a weak but significant apical Cu–S(Met) bond as a consequence of the conformational change signaled by the shift in the C–S(Cys) stretching frequency. Such a weak bond would inhibit large-amplitude motions of the copper atom perpendicular to the N_2S(Cys) plane, which are permitted at room temperature due to the virtual absence of a Cu–S(Met) bond[9,14] and which result in the facile dephasing of the modes associated with the in-plane structure. These considerations may have profound affects upon the quantum dynamics of electron transfer.

Table IX. Integrated Peak Intensities[a] of Principal RR Features of Single-Copper Blue Proteins (12 K)

azurin (PA)[b] peak, %A	stellacyanin[c] peak, %A	plastocyanin (spinach)[d] peak, %A
G, H, 3.0, 4.4	D, 5.4	B, 8.4
L, 14.9	F, 16.1	
	G, 11.4	F, 15.0
		G, 10.6
M, 15.5	H, 8.6	H, 9.5
		I, 9.1
N, 27.7	I, 32.8	J, 32.3
	K, 7.4	
O, 16.5	L, 5.6	
P, 3.9	M, 3.4	K, 14.7

[a] Expressed as percent of total peak area between 200 and 500 cm^{-1} for each protein. [b] 50% Gaussian, 50% Lorentzian peak shape. [c] 75% Gaussian, 25% Lorentzian peak shape. [d] 100% Lorentzian peak shape.

The RR spectra of spinach and bean plastocyanins are subtly different. At 12 K, notable differences include better resolution of peaks J (425 cm^{-1}) and K (442 cm^{-1}) in spinach plastocyanin. In bean plastocyanin, peak J is at higher frequency and peak K is at lower frequency (427 and 440 cm^{-1}, respectively), suggesting a possible coupled-oscillator relationship between these features. As temperature is lowered, the C–S(Cys) stretch upshifts by 14 cm^{-1} (from 753 to 767 cm^{-1}) in spinach plastocyanin as noted above and elsewhere.[14] In bean plastocyanin, this upshift is only 7 cm^{-1} (762–769 cm^{-1}), suggesting a smaller change in the $(Cu–S–C_\beta)–(S–C_\beta–C_\alpha)$ dihedral angle with temperature in the bean protein. Concomitant with the smaller change in dihedral angle in bean plastocyanin, we note that the change in peak width with temperature in this protein is also less pronounced than for spinach plastocyanin. In the context of the above interpretation of these phenomena, this suggests a stronger Cu–S(Met) interaction at room temperature in bean plastocyanin than in spinach.

The poplar plastocyanin RR spectrum is qualitatively similar to both bean and spinach (Table V). Thus, there are no major differences among the plastocyanin structures at low temperature.

We noted previously[14] that the overtone/combination regions of plastocyanin are dominated by unresolved combinations, that the first overtone of the strongest fundamental appears only as a weak shoulder, and that the combinations observed apparently involve virtually every permutation of the fundamentals rather than only the most intense one as is the case in PA azurin and stellacyanin. It appears that Duschinsky mixing in the excited state of plastocyanin is extreme, creating many strong combinations. At the same time, it appears that the overtone intensities are damped by multimode effects. Like the facile dephasing at room temperature, this may be an effect of a three-coordinate geometry of Cu(II) in the ground state of plastocyanin, which may allow a large geometry change in the excited state (e.g., substantial bonding of the excited state "Cu(I)" to methionine) and hence excited-state normal modes which differ greatly from the ground state.

Oxidases. The oxidases tree laccase, fungal laccase, ascorbate oxidase, and ceruloplasmin are considered together primarily because of their functional similarities. They all contain type 1 (blue), type 2 ("normal"), and type 3 (paired) copper. Because relative peak intensities differ considerably among these proteins, it is not obvious from simply viewing the spectra (Figures 6 and 7) that any relationship exists among them. Table VI, however, reveals that there is a peak-for-peak correlation of the frequencies of the major features in the spectra of tree laccase, fungal laccase, and ascorbate oxidase. This correlation does not extend to ceruloplasmin, either in appearance of the spectra or in frequencies. For the laccases, this similarity has been noted by others.[20]

We pointed out in the stellacyanin discussion how a relatively weak (long) Cu–S bond results in a low natural frequency of the Cu–S stretch. Owing to the ground-state distribution of the Cu–S(Cys) stretch, the RR intensity due to the Cu–S(cys) coordinate in stellacyanin occurs in lower-frequency normal modes. Apparently, this effect is operating among the laccases and ascorbate oxidase. The intensity patterns suggest that the Cu–S bond is weakest (longest) for tree laccase and strongest (shortest) in fungal laccase. Furthermore, the very similar frequencies in these three proteins suggest that the structures of the type 1 copper sites in these oxidases are virtually identical, except for the Cu–S(Cys) bond length. Our results on the azurins and plastocyanins demonstrate that subtle structural alterations result in considerably different RR frequencies. Conversely, similar frequency patterns suggest similar vibrational interactions and by inference similar structures.

There is considerable (though less pronounced) similarity between the laccase/ascorbate oxidase spectra and those of the plastocyanins. The number of intense features in the 350–450-cm^{-1} range and their frequencies are similar. The C_β–S stretch (peak V, Table VI) in tree laccase exhibits a similar upshift in frequency with decreasing temperature. The overtone/combination regions are similar in that (for tree laccase and ascorbate oxidase) combinations are numerous and dominant in intensity. The overtone region of fungal laccase has a different appearance due to the high frequency and dominant intensity of the fundamental peak N.

Temperature-dependent changes are observed in the spectra of the laccases which are unusual among the blue copper proteins and which we do not understand at present. Notably, mode-dependent line-width changes and intensity swapping between peaks J and L occur. Nevertheless, we infer a generic similarity between the structure of the copper sites in plastocyanin and in laccase/ascorbate oxidase.

In essence, the RR spectrum of ceruloplasmin (Figure 6) is like that of AF azurin, except that peak L in ceruloplasmin is resolved into peaks N and O in AF. Peak L is abnormally broad and must contain more than one component. Another possible reason for poor resolution of these features in ceruloplasmin is that the RR frequencies of the two type 1 copper sites in ceruloplasmin may differ. Points of similarity between ceruloplasmin and azurin (see Figures 1 (300 K) and 2, Table I) include the frequencies and relative intensities of the modes near 270 cm^{-1} (peaks G and H in azurin, peaks E and F in ceruloplasmin), the frequencies and relative intensities of all prominent features in the 340–500-cm^{-1} range, the presence of the 657-cm^{-1} fundamental which is peculiar to the azurins and ceruloplasmin, the frequency of the C_β–S(Cys) stretch, and the appearance of the overtone region at room temperature (see Figure 1). We infer a close generic similarity between the azurin structure and the type 1 sites of ceruloplasmin.

Rack-Induced Bonding

In a recent note,[12] two of us have drawn attention to the relationship between ligand-field strengths and electron-transfer enthalpies for blue copper proteins whose electron-transfer entropies are not very different. To accommodate this relationship over a 50 kJ mol^{-1} range of $\Delta H°$ values and at the same time understand why the intense S(Cys) → Cu($d_{x^2-y^2}$) transition always falls in the 600-nm region, it was proposed that the key electronic tuning mechanisms is a variation in π back-bonding at the blue copper site. Increasing the π-acceptor strength of the copper ligands would enhance the ligand field and stabilize the reduced (Cu(II)) state of the system, in accord with observation.

Because unconstrained ligands on their own could hardly manipulate their π-acceptor interactions with copper in the described fashion, a structure-forcing, peptide-backbone rack mechanism was invoked. In the present context, this mechanism could be called rack-induced bonding, meaning simply that the protein-shaped binding site can be adjusted to stabilize copper(I) to varying degrees. One key spectroscopic indicator of this preferential stabilization is an increased ligand field at the *oxidized* copper.

Sulfur ligands are obvious candidates for rack-induced bonding in the case of blue copper. Systematic variation in the S(Met)–Cu or S(Cys)–Cu interaction, or more likely some combination of the two, could tune the electron-transfer enthalpies in the manner observed. An attractive model involves *both* Cu–S distances decreasing as the electron-transfer enthalpies become more negative (corresponding to the $E°$ values increasing) in classical synergistic fashion. The role of S(Met) would be to remove excess electron density via π back-bonding as the stronger donor S(Cys) moves closer to the Cu. A clear prediction of this model is that the Cu–S(Cys) stretching frequency will increase as the electron-transfer exothermicity increases.

Evidence presented in previous sections suggests that the main source of RR intensity in the vibrations of the blue copper chromophore is the fractional contribution to each vibration by the Cu–S(Cys) stretching coordinate. To the extent that this is a valid approximation, it is possible to use the RR intensities to calculate the fraction of the excited-state coordinate displacement (assumed to be only a change in Cu–S(Cys) bond distance) which is projected upon each ground-state normal vibrational coordinate. This in turn is identical with the contribution to each ground-state normal coordinate by the Cu–S(Cys) stretch. Further assuming that the reduced masses of all RR modes are approximately equal, the relative contributions of the Cu–S(Cys) stretch to each ground-state mode can be calculated from a slightly rearranged version of eq 3 (recall that V_k' = (force constant for coordinate k)·$(\Delta q)_k$):

$$[(I_{01}{}^k)(\nu_k)]/[(I_{01}{}^l)(\nu_l)] = [\Delta r(\text{Cu–S})_k \Delta r(\text{Cu–S})_l]^2 \quad (5)$$

In eq 5, $\Delta r(\text{Cu–S})_k$, for example, is the excited-state displacement of the Cu–S(Cys) bond projected on ground-state normal mode k. Since frequencies scale as energy which in turn scales as displacement squared, the "natural frequency" of the Cu–S(Cys) bond as a local oscillator may in turn be estimated according to eq 6.

$$\nu_{\text{Cu-S}} = \sum_i [(I_{01}{}^i)(\nu_i)^2] / \sum_i (I_{01}{}^i)(\nu_i) \quad (6)$$

The results of the calculation based on eq 6 are presented in Table X, along with the relevant ligand field and thermodynamic parameters. Agreement between the local oscillator Cu–S(Cys) frequencies and the electron-transfer enthalpies for the four proteins for which $\Delta H°$ has been determined is essentially linear (see Figure 8), a strikingly good correlation considering the assumption that all the RR intensity is due to the distribution of the Cu–S(Cys) stretching potential among the observed normal modes. For the remaining proteins for which only $E°$ information is known, good agreement among $\nu_{\text{Cu-S}}$, Δ_{LF}, and electron-transfer free energy is indicated. Thus, the RR data provide independent confirmation that rack-induced bonding is a key feature of the description of the copper sites.

The local oscillator Cu–S frequencies can be employed to estimate the quantitative influence of the rack mechanism upon the Cu–S(cys) bond distances in the various proteins. Empirical relationships such as Badger's rule and more recent expressions by Herschbach and Laurie[29] allow calculation of bond distance changes in a series of similar structures if a vibrational frequency associated with a particular bond can be identified. The relevant expression and the resulting calculated $r_{\text{Cu-S}}$ values (employing the plastocyanin bond distance and local oscillator Cu–S frequency as reference values) are given in Table X. It is noteworthy that

Table X. "Local Oscillator"[a] Cu-S Stretching Frequencies, Ligand-Field Energies (Δ),[b] Cu-S Bond Distances, and Thermodynamic Parameters[c] for Blue Copper Proteins

protein	ν(Cu-S), cm^{-1}	Δ, kJ mol^{-1}	r(Cu-S), Å exptl (calcd)[d]	$\Delta H°/\Delta S°$, kJ mol^{-1}/(J mol^{-1} K^{-1})	$E°$, mV vs. NHE
stellacyanin	386	44.2	2.19[e] (2.17)	-41.5/-17.6	191
tree laccase	402	71.8	(2.13)		394
plastocyanin	403	59.8	2.13[f] (2.13)	-58.2/-10.1	360
azurin	405	69.4	2.1[g] (2.13)	-70.9/-67.6	308
ascorbate oxidase	408	69.4	(2.12)		
ceruloplasmin	409	73.0	(2.12)		490, 580
fungal laccase	421	86.7	(2.09)	-92.3/7.1	785

[a] Calculated from observed RR frequencies and intensities (see text). [b] Energy of the lowest d-d transition (see ref 5 and 12). [c] See ref 12 and 30 and literature cited therein. [d] Calculated from [r-r(ref) = 1.96 log (ν(ref)/ν)], ref 29. [e] Reference 11. [f] Reference 6. This Cu-S distance was used as r(ref) and the plastocyanin frequency was used as ν(ref). [g] References 7 and 8.

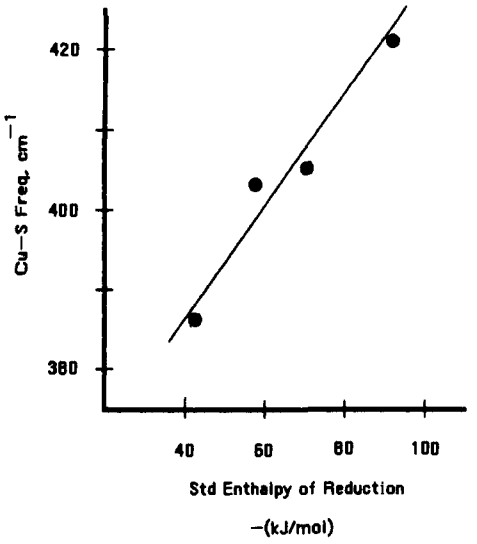

Figure 8. Correlation of the standard enthalpy ($\Delta H°$) for the reduction of the Cu^{2+} form of the proteins stellacyanin (leftmost point), plastocyanin, azurin, and fungal laccase (rightmost point) with the frequency of the Cu-S(Cys) bond as a local oscillator (see text).

the calculated value of the stellacyanin Cu-S distance, 2.17 Å, is in good agreement with the distance determined experimentally by EXAFS (2.19 Å). We may confidently predict that the rack mechanism forces shortening of the Cu-S bond in fungal laccase to a value near 2.09 Å.

Concluding Remarks

The RR spectral characteristics of the blue copper centers of the proteins examined are typified by the three single-copper proteins plastocyanin, azurin, and stellacyanin. The key features of plastocyanin appear from the crystal structure and the RR data to be the availability of a maximum of four donors to coordinate to copper, the effective coordination of only three of these under at least some conditions, and large excited-state structural changes resulting in strong Duschinsky mixing as evidenced by the RR overtones and combinations. Azurin may have four or possibly five donors in the vicinity of copper.[7,8] The RR data suggest that certain motions of the copper atom are constrained compared to plastocyanin. We have previously suggested[14] that this is because the copper atom is under all conditions coordinated to at least four of the proximate donors. Azurin shows the weakest Duschinsky effect of all the blue copper systems, as evidenced by the intensities of the overtones and combinations. This suggests that the excited-state structure is not grossly different from the ground state in azurin, reinforcing the idea of a somewhat constrained copper site. Stellacyanin alone lacks methionine. Some form of interaction of a *protonated* peptide group with the blue copper chromophore is indicated. Duschinsky effect in stellacyanin is somewhat stronger than it is in azurin.

Among the proteins examined, subtle structural parameters clearly vary with readily observable effects on the frequencies and intensities of correlated RR modes. These parameters, which include but are not limited to the Cu-S(Cys) distance and apical bonding interactions, are subject to control by the overall protein structure. Any of them may modulate the biological function of the protein by affecting the thermochemistry or quantum dynamics of the electron-transfer function of the blue copper site.

Acknowledgment. We are grateful for support of this work by the United States Public Heath Service (NIH Grants GM 22432 to S.I.C. AM 19038 to H.B.G., and AM 33679 to W.H.W.), the Swedish Natural Science Research Council (to B.G.M.), and the Robert A. Welch Foundation (Grant F-733 to WHW). K.A.N. was recipient of an NIH Postdoctoral Fellowship (AM 06966).

Portions of this work were performed at the Los Alamos National Laboratory under the auspices of the U.S. Department of Energy (BIS).

Finally, we are grateful to Rick Heller, Tom Loehr, Vince Miskowski, Lisa Nestor, Tom Spiro, and Dave Tannor for a number of stimulating and helpful discussions.

Registry No. ^{65}Cu, 14119-06-3; D_2, 7782-39-0; ^{63}Cu, 14191-84-5; S, 7704-34-9; Cu, 7440-50-8; ascorbate oxidase, 9029-44-1; ceruloplasmin, 9031-37-2; laccase, 80498-15-3.